

17 **Abstract**

18 In this study, we present a molecular characterization of the interaction between the
19 SARS-CoV-2 envelope protein E with TLR2. We demonstrated that E protein interacts
20 physically with TLR2 receptor in a specific and dose-dependent manner. Furthermore, we
21 showed that this interaction is able to engage TLR2 pathway as demonstrated by its capacity
22 to activate NF- κ B transcription factor and to stimulate the production of CXCL8
23 inflammatory chemokine in a TLR2-dependent manner. Furthermore, in agreement with the
24 importance of NF- κ B in TLR signaling pathway, we showed that the chemical inhibition of
25 this transcription factor led to significant inhibition of CXCL8 production, while blockade of
26 P38 and ERK1/2 MAP kinases resulted only in a partial CXCL8 inhibition. Overall, our
27 findings suggest considering the envelope protein E as a novel target for COVID-19
28 interventions: (i) either by exploring the therapeutic effect of anti-E blocking/neutralizing
29 antibodies in symptomatic COVID-19 patients, or (ii) as a promising non-Spike SARS-CoV-2
30 antigen candidate to include in the development of next generation prophylactic vaccines
31 against COVID-19 infection and disease.

32

33 **Importance**

34 Although, the exact mechanisms of COVID-19 pathogenesis are unknown, recent data
35 demonstrated that elevated levels of pro-inflammatory cytokines in serum is associated with
36 enhanced disease pathogenesis and mortality. Thus, determining the molecular mechanisms
37 responsible for inflammatory cytokine production in the course of SARS-CoV-2 infection
38 could provide future therapeutic targets. In this context, to the best of our knowledge, our
39 report is first to use a detailed molecular characterization to demonstrate that SARS-CoV-2
40 Envelope E protein binds to TLR2 receptor. Specifically, we showed that SARS-CoV-2
41 Envelope E protein binds to TLR2 in a direct, specific and dose-dependent manner.
42 Investigating signalling events that control downstream activation of cytokine production
43 show that E protein / TLR2 binding leads to the activation of NF- κ B transcription factor that
44 control the expression of multiple pro-inflammatory cytokines including CXCL8. Overall, our
45 findings suggest considering the envelope protein E as a novel target for COVID-19
46 interventions.

47 **1. Introduction**

48 SARS-CoV-2, the etiologic agent of the current worldwide COVID-19 pandemic, is a
49 β -coronavirus belonging to the Coronaviridae family. SARS-CoV-2, emerged in 2019, is the
50 third causative agent of severe acute respiratory syndrome also named COVID-19
51 (CoronaVirus Disease 2019). The two other viruses are SARS-CoV-1 and MERS-CoV
52 emerged in 2003 and 2012, respectively. SARS-CoV-2 is an enveloped virus with a single
53 strand positive RNA genome of about 30 kbases and shares 79% of nucleotide identity with
54 the genome of SARS-CoV (1). Its envelope contains three proteins. i) The "Spike" protein (S)
55 a glycoprotein of 180–200 kDa (2), present as trimers at the surface of the viral particle. It
56 plays a crucial role in the virus entry into target cells following its interaction with ACE2
57 receptor to induce viral and cell targets membranes fusion (3). ii) The Membrane protein (M),
58 a protein of 25–30 kDa, involved in viral assembly, is the major protein of the envelope. iii)
59 The Envelope Protein (E), is a 8.4-12 kDa polypeptide of 76 to 109 amino-acids (4, 5). It is a
60 small integral viral membrane protein. Inside infected cells, E protein is localized in the RE,
61 Golgi and ERGIC (ER/Golgi intermediate compartments) where it seems to play an important
62 role in the virus assembly and budding (6, 7). In agreement with its role in viral assembly and
63 budding at the RE/Golgi, compartment where are produced the complete viral particles at the
64 end of coronavirus life cycle, its mutation or deletion leads to a substantial decrease in the
65 capacity of viral replication (8, 9). Thus, the important role of E protein, makes it as potential
66 target for antiviral drug molecules and vaccine candidates development (10). Protein-protein
67 interactions were well characterized between E and M proteins, as shown by the presence of
68 E-M complexes at the level of ERGIC in infected cells (11, 12). It is also interesting to note
69 that the expression of these two proteins is sufficient for the formation of VLP (viral like
70 particles) (6, 13). By interfering with protein transport via secretory pathways and with the
71 normal function of the immune system, E protein could act as a pathogenic factor in the
72 immunopathogenesis associated with SARS-CoV, MERS-CoV and SARS-CoV2 (8, 14). In
73 fact, in SARS-CoV infected cells, E protein anchored to a lipid bilayer is able to adopt a
74 structure forming membrane-integral pores, also named viroporin, with a selective activity for
75 cations including, H⁺, K⁺, Na⁺ and Ca²⁺ (15). At least, the selective permeability to Ca²⁺
76 has been reported to be associated with the inflammatory response often observed in ARDS
77 (acute respiratory distress syndrome) (15).

78 Infection with SARS-CoV-2 is accompanied by deregulation of the control
79 mechanisms of the innate immune response (16, 17). This deregulation is characterized by a

80 delay in the IFN-I and III production and also by an exacerbation of the inflammatory
81 response including, IL-6, TNF- α , IL-1 β , IFN- γ but also certain chemokines including CXCL8
82 (18). In patients developing a critical COVID-19, this dysregulation leads to the establishment
83 of a cytokine storm, a deleterious proapoptotic state for various tissues and organs including
84 the lungs (19-21). SARS-CoV-2 infection also impact the adaptative immune response by
85 affecting the normal physiological functions of antigenic presenting cells (22), but also CD4+,
86 and in a higher degree CD8+ T-cells(23, 24).

87 Understanding the molecular mechanisms responsible, on one hand, for the control or
88 escape of SARS-CoV-2 detection by innate immune sensors and, on the other hand, for
89 SARS-CoV-2-induced pathological hyper-inflammation are essential steps for the
90 development of effective therapeutic strategies against COVID-19. To achieve this goal, it is
91 important to determine the nature of viral PAMPS and cellular PRRs that are engaged in the
92 course of SARS-CoV-2 infection. According to their biochemical and structural
93 characteristics, PRRs are classified into six different families including: (i) Toll-Like
94 Receptors (TLRs); (ii) Lectin type C receptors (CLR); (iii) scavenger receptors; and (iv) the
95 opsonin receptors. In addition to these transmembrane receptors, found on the surface of the
96 cell or in endosomes, cells also express cytosolic and/or nuclear receptors including: (v)
97 receptors for nucleic acids, RLR (RIG-I-Like), which recognize the RNAs and cytosolic DNA
98 sensors called CDS, including cGAS, and AIM2-like receptors (ALRs) including AIM2, and
99 (vi) NOD type receptors, NOD-Like (NLRs) (25, 26). To date, at least nine PRRs have been
100 reported in the detection of RNA viruses including, TLR7 and 8 (single-stranded RNA),
101 TLR3 (single-stranded RNA), RIG-I and MDA-5 (single and / or double-stranded RNA, di or
102 tri-phosphorylated in 5'), DAI / ZBP-1 (RNA with a Z conformation)(27, 28), receptors
103 forming NLRP3 and NLRP1(29) inflammasomes, as well as helicases of the DDX family
104 including DDX3 which recognizes the RNA of HIV-1(30). More recently, it was advanced
105 that SARS-CoV-2 E envelope protein can be sensed by TLR2 (31), and its expression, as that
106 of its cofactor MyD88, and the induced inflammatory responses seem to increase more
107 importantly in patients with critical severe COVID-19 (32). More interestingly it was shown,
108 in ACE2 transgenic mouse model, that the blockade of TLR2 pathway allowed protection
109 against the disease development and lethality induced by SARS-CoV infection (32).

110 Considering the important role of innate immune sensors, including TLR2, as potential
111 therapeutic targets in order to alleviate the development of hyper-inflammation and cytokine
112 storm associated with severe COVID-19, in the present study we analysed at molecular level,
113 the interaction between SARS-CoV-2 envelope protein E and human TLR2. Our findings

114 demonstrated that the SARS-CoV-2 E protein interacts with TLR2 receptor in a specific and
115 dose dependent manner in a solid-phase binding assay but also on the cell membrane of TLR2
116 positive cells, including primary human monocytes and macrophages. Moreover, using HEK-
117 based TLR2 reporter cell lines, we also showed that E protein activates TLR2 signaling
118 pathway that culminate in the activation of NF- κ B transcription factor and production of
119 inflammatory cytokines/chemokine including CXCL8.

120 The finding suggest considering the envelope protein E as a novel target for COVID-
121 19 interventions: (i) either by exploring the therapeutic effect of anti-E blocking/neutralizing
122 antibodies in symptomatic COVID-19 patients, or (ii) as a promising non-Spike SARS-CoV-2
123 antigen candidate to include in the development of next generation prophylactic vaccines
124 against COVID-19 infection and disease.

125

126

127

128 **2. Materials and Methods**

129

130 ***2.1 Ethics statement:***

131 The use of human cells in this study was approved by the Research Ethical Committee
132 of Haute-Garonne, France. Human Peripheral Blood Mononuclear Cells (PBMC) were
133 isolated from buffy coat of healthy human donors. Buffy coats were provided anonymously
134 by the EFS (Etablissement Français du Sang, Toulouse, France). Written informed consent
135 was obtained from the donors under EFS contract N° 21/PVNT/TOU/INSERM01/2011-0059,
136 according to French Decree N° 2007–1220 (articles L1243-4, R1243-61).

137

138 ***2.2 Cells:***

139 Human embryonic kidney cell lines stably transfected with TLR2 (HEK-TLR2), TLR4
140 (HEK-TLR4) and HEK-TLR2-blue and control HEK cell line (HEK-null) were purchased
141 from InvivoGen and cultured in DMEM supplemented with 10 % FCS, 1% of P/S and
142 selections antibiotics according to the manufacturer's instructions (InvivoGen). Vero E6 and
143 A549 cell lines were cultured in DMEM supplemented with 10% FCS and 1% of P/S.

144

145 ***2.3 Virus infection:***

146 Primary monocytes-derived macrophages (10^6 cells) were treated with 0.01 to 1 MOI
147 of the mNeonGreen SARS-CoV-2. This recombinant reporter SARS-CoV-2 developed by Pei
148 Yong Shi et al (33) was obtained from World Reference Center for Emerging Viruses and
149 Arboviruses (WRCEVA).

150

151 ***2.4 Isolation of human monocytes:***

152 PBMCs were isolated from buffy coats of healthy blood donors (from Etablissement
153 Français du Sang [EFS], Toulouse) and monocytes were separated from lymphocytes by
154 positive selection using magnetic cell sorting technique according to the manufacturer's
155 instructions (Miltenyi Biotec) and as described (34).

156

157 ***2.5 Generation of monocyte-derived macrophages:***

158 To allow differentiation of monocytes into monocyte-derived macrophages,
159 monocytes were cultured in DMEM medium (Invitrogen) supplemented with 10% fetal calf
160 serum (FCS) 100 IU/ml penicillin, 100 µg/ml streptomycin, 10 ng/ml GM-CSF, and 10 ng/ml

161 MCSF. After 3 days of culture, cells were stimulated by the same amount of GM-CSF and M-
162 CSF and cultured for additional 4 days before their use in our experiments as differentiated
163 macrophages.

164

165 ***2.6 Chemical products, Proteins, and Antibodies:***

166 PAM₂CSK₄, PAM₃CSK₄, LPS-RS were purchased from InvivoGen. Recombinant
167 soluble E protein from SARS-CoV-2 was purchased from Clinisciences. GST, GST-Nef and
168 the corresponding antibodies were produced in our laboratory. Soluble recombinant TLR2
169 was purchased from R&D systems. Anti-TLR2 and anti-TLR4 monoclonal antibodies were
170 obtained from eBioscience. Anti-Phospho-P65 and anti-total P65 were purchased from cell
171 Signalling. Bay11-7082, SB202190, PD98059 and RO318220 were purchased from
172 Calbiochem.

173

174 ***2.7 Interaction of E protein with TLR2 in a solid phase assay:***

175 The binding of the recombinant E-GST protein with TLR2 was tested in a solid phase
176 assay. Briefly, 100 µL of recombinant soluble TLR2 (R&D systems) at 1 µg / ml are coated
177 during 2 hours at room temperature in 96-well plates. After 1 hour of saturation with 300 µL
178 of PBS containing 5% non-fat milk and 5 washes with PBS-Tween 0.05%, 100 µL of
179 different concentrations of the soluble protein E-GST (1ng- 1000 ng/ml) are added to each
180 well. After 1 hour of incubation at 37 °C, 5 washes were performed with PBS-0.05% Tween.
181 Then, the detection of TLR2-E-GST complexes were performed by an additional incubation
182 during 1 hour at room temperature with 100µl of a rabbit anti-GST sera previously diluted at
183 1/500 in PBS-tween 0.05% containing 5% non fat milk. After 5 further washes, the complexes
184 TLR2-E-GST-anti-GST were labeled by 1 hour incubation at room temperature with 100 µl
185 of anti-rabbit IgG antibodies coupled to horseradish peroxidase in PBS-tween 0.05%
186 containing 5% non-fat milk (DAKOTA). After a last 5 washes with PBS-tween 0.05%,
187 TLR2-E-GST-anti-GST-anti-rabbit-IgG-peroxydase complexes were revealed by the addition
188 of 100 µL of TMB substrate (Tetramethylbenzidine). After 15 to 30 min incubation, the
189 peroxidase reaction was stopped with 50 µL of sulfuric acid (2N) and then the optical density
190 was read at 450/570 nm.

191

192 ***2.8 Inhibition assay of E-TLR2 interaction:***

193 The specificity of E-TLR2 interaction was evaluated in a solid phase binding assay as
194 described above except that various amounts of PAM₂CSK₄, PAM₃CSK₄ were added to

195 rTLR2-precoated wells during 1 hour before adding a constant amount of soluble E protein
196 (200ng).

197

198 ***2.9 Flow cytometry analysis:***

199 Monocytes (10^6) were incubated with GST or GST-E SARS-CoV-2 protein at 0.1-
200 10 μ g/ml for 1 hour at 37 °C in PBS, BSA 0.5%, NaN₃ 0.05%. Then, cells were washed 3
201 times with PBS, BSA 0.5%, NaN₃ 0.05% to remove unbound proteins. Cells were stained
202 with and anti-GST-Alexa 488 (Catalog # A-11131, ThermoFisher, 1/2000) during 1 hour at
203 room temperature and washed 3 times with PBS, BSA 0.5%, NaN₃ 0.05%. Then cells were
204 fixed with PFA 4%. Data were acquired using FACSCalibur (BD).

205

206 ***2.10 Microscopy analysis:***

207 The analysis of the binding of E protein to macrophages was analyzed by microscopy.
208 To this end macrophages (10^6) were incubated with GST or GST-E SARS-CoV-2 protein at
209 10 μ g/ml for 1 hour at 37°C PBS, BSA 0.5%, NaN₃ 0.05%. Then, cells were washed 3 times
210 with PBS, BSA 0.5%, NaN₃ 0.05% to remove unbound proteins. Then cells were washed 3
211 times with PBS, stained with Hoechst, and anti-GST-Alexa 488 (1/500) during 1 hour at room
212 temperature and washed 3 times with PBS, BSA 0.5%, NaN₃ 0.05%. Finally, cells were fixed
213 with PFA 4% before imaging. Images were acquired using EVOS M700 (Invitrogen) at 40x
214 magnification.

215

216 ***2.11 Cell based biological assays:***

217 Primary human monocytes or macrophages cells (10^6 cells) or HEK-null, HEK-TLR2
218 or HEK-TLR4 cell lines (2,5. 10^5 cells) were plated in 24 well plates and treated by E protein
219 or PAM₃CSK₄ and PAM₂CSK₂ as positive controls at the indicated concentrations. Untreated
220 cells were used as negative controls. To block TLR2, anti-TLR2 were added in cell culture
221 medium 1 hr before treatment with E protein. To inhibit cell signaling pathways, cells were
222 incubated with chemical inhibitors 30 minutes before treatment with E protein. To inhibit the
223 binding of E protein to cell membrane TLR2, E protein (at 200ng/ml) was preincubated with
224 rTLR2 (20 ng/ml) during 1 hour at RT, before being added to HEK-TLR2 cells. Cell
225 supernatants were collected 18hrs after E-treatment and frozen at -20°C before further
226 analysis.

227

228 ***2.12 Phosphorylation analysis of NF-kB P65 subunit and Western blot analysis:***

229 HEK-TLR2 cells ($2.5 \cdot 10^5$ cells) were treated during 30 or 60 min with E protein (1
230 $\mu\text{g/ml}$) or, with GST ($1\mu\text{g/ml}$) or PAM₃CSK₄ (10 ng/ml) as negative and positive controls
231 respectively. Then, cells were lysed and prepared for immunoblot as previously described
232 (35).

233

234 ***2.13 NF- κ B assay using HEK-TLR2-Blue:***

235 The capacity of E protein to activate NF- κ B was tested by using HEK-TLR2-blue
236 (InvivoGen). In this assay, HEK-TLR2 cells stably transfected with SEAP (secreted
237 embryonic alkaline phosphatase) gene under the control of NF- κ B promoter were plated at
238 $2.5 \cdot 10^5$ cells per well in 24 well plates one day before the experiment. The following day cells
239 were treated by E protein in cell culture medium at the indicated concentration. 18 hrs after
240 treatment, supernatants were collected and quantification of SEAP was performed according
241 to manufacturer's instructions (InvivoGen).

242

243 ***2.14 CXCL8 quantification by ELISA:***

244 Cells were stimulated with various amount of E protein ($1\text{-}1000\text{ng/ml}$). After 18 hours
245 of stimulation at 37°C , supernatants were harvested and stocked at -20°C until CXCL8
246 quantification by ELISA kits according the instructions of the manufacturer (R&D system).

247

248 ***2.15 Statistical analyses:***

249 Statistical analysis was performed using GraphPad Prism software v.5. All results are
250 expressed as means \pm SD. All experiments were performed a minimum of three times.
251 Differences in the means for the different groups were tested using one-way ANOVA
252 followed by Bonferroni post hoc test. A p-value <0.05 was considered statistically significant.
253 Statistical significance comparing different groups is denoted with * for $p < 0.05$, ** $p < 0.01$,
254 *** $p < 0.001$, ns non-significant.

255

256

257 **3. Results**

258 ***3.1 SARS-CoV-2 E-envelope protein interacts directly and physically with TLR2:***

259 In order to analyse the capacity of SARS-CoV-2 envelope protein E to interact with
260 TLR2 at a molecular level, we tested in a solid phase assay the binding of various amounts of
261 E protein (1 ng/ml-1000 ng/ml) to a constant amount of pre-coated human recombinant TLR2
262 (1 µg/ml). The obtained results depicted in **Figure 1** showed that E protein binds in a dose-
263 dependent manner to TLR2. In contrast, no significant binding to TLR2 was observed when
264 the experiment was performed with GST, instead of E protein (**Figure 1A**). Further, we also
265 showed that E protein, but not GST used as control, is also able to bind to human primary
266 monocytes when analysed by flow cytometry (**Figure 1B, C**) and to human primary
267 macrophages when analysed by microscopy (**Figure 1D**).

268 Altogether, these results demonstrate that the SARS-CoV-2 envelope protein is able to
269 interact physically, in a dose-dependent manner with the human soluble recombinant TLR2
270 but also with cell membrane TLR2 expressed at the surface of primary human monocytes and
271 macrophages.

272 ***3.2 PAM₂CSK₄ and PAM₃CSK₄ antagonise SARS-CoV-2 E protein binding to TLR2:***

273 PAM₂CSK₄, a synthetic diacylated lipopeptide ligand of TLR2/TLR6, and
274 PAM₃CSK₄, a synthetic triacylated lipopeptide ligand of TLR2/TLR1 have been historically
275 characterized as the first identified ligands of TLR2. Thus, in order to characterise the
276 specificity of the interaction of E protein with TLR2, we evaluated the capacity of these two
277 ligands PAM₂CSK₄ and PAM₃CSK₄ to inhibit E-TLR2 interaction. To this end, the
278 experiment was performed as described in figure 1, by using a constant concentration of E
279 protein (200ng) but in presence of escalating amounts of PAM₂CSK₄ or PAM₃CSK₄ (0.1µM
280 to 10µM). Both ligands inhibited E-TLR2 interaction in a dose dependent-manner (**Figure**
281 **2A-B**). However, only a partial inhibition, exceeding 50%, was obtained with PAM₂CSK₄ and
282 PAM₃CSK₄ used at 10µM. Thus, these characterizations demonstrate that E protein-TLR2
283 interaction is specific as demonstrated by the capacity of PAM₂CSK₄ and PAM₃CSK₄ to
284 inhibit this interaction.

285 ***3.3 SARS-CoV-2 E Protein stimulates the production of CXCL8 inflammatory chemokine*** 286 ***by recruiting TLR2 pathway:***

287 In order to study the biological consequences of E-TLR2 interaction, we tested the
288 capacity of E protein to stimulate the production of CXCL8 in a HEK cell lines-based assay
289 using cells stably transfected with the human TLR2 (HEK-TLR2) or TLR4 (HEK-TLR4)
290 receptors or HEK-null (transfected with empty plasmid). As previously shown by our group,
291 activation of TLR-dependent pathway in HEK cells lines stimulates the production of
292 measurable amount of CXCL8 chemokine, while other TLR-dependent cytokines including
293 TNF- α , IL-6, IL-10 were barely detectable. As consequence, the production of CXCL8 by
294 HEK cells lines was used as a marker of TLR response (36). Results presented in figure 3A
295 show that E protein from SARS-CoV-2 (200ng/ml) stimulates the production of CXCL8 in
296 TLR2-expressing HEK cell lines, while GST or GST-Nef, two unrelated SARS-CoV-2 gene
297 products, used as controls, do not stimulate significant production of CXCL8 when used at
298 concentrations up to 1 μ g/ml (**Figure 3A**). As additional controls, no production of CXCL8
299 was obtained in the supernatants of unstimulated HEK-TLR2 cell line, while a clear
300 production of CXCL8 was produced following the stimulation by the synthetic ligand of
301 TLR2 PAM₃CSK₄ (**Figure 3A**). The specificity of the activation of TLR2 pathway by E
302 protein was further demonstrated by showing that E protein induced the production of CXCL8
303 in a dose-dependent manner, with the lowest amount of E protein giving a detectable CXCL8
304 production being around 10 ng/ml (**Figure 3B**). The specificity of E-TLR2 pathway activation
305 was further supported by the fact that no CXCL8 production was obtained in HEK-null cell
306 (**Figure 3C**) nor in HEK-TLR4 (**Figure 3D**) cell lines. This latter control also demonstrated
307 the absence of endotoxins contaminants in our recombinant E protein as demonstrated by the
308 absence of any activation of TLR4 pathway (**Figure 3C-D**).

309 Taking into account the data obtained with HEK-TLR2 cell line, we tested the
310 capacity of E protein to activate the production of CXCL8 in human primary monocytes and
311 macrophages. To this end, human monocytes and macrophages were stimulated by increasing
312 concentrations of E protein (1 ng/ml to 200 ng/ml) for 20 hours and CXCL8 was quantified
313 by ELISA as described above. The obtained results showed that E protein stimulated the
314 production of CXCL8 in both primary human monocytes and macrophages (**Figure 3E**).

315 In line with these results, we also showed that treatment of primary human
316 macrophages, during 20 hours, with infectious SARS-CoV-2 viral particles also resulted in
317 the production of CXCL8 in cell supernatants (**Figure 3F**). It is interesting to note that
318 macrophages do not show any signs of viral replication, as shown by the absence of
319 NeonGreen fluorescence in macrophages when infected with the recombinant mNeonGreen

320 SARS-CoV-2, used at 0.01, 0,1 and 1 MOI (**Supplementary Figure S1**). As positive control,
321 we showed that the treatment of VeroE6 cells with the recombinant mNeonGreen SARS-
322 CoV-2 resulted in a clear infection of these cells (**Supplementary Figure S1**).

323 Altogether, our results showed that SARS-CoV-2 E protein, by recruiting, at least,
324 TLR2 pathway stimulated the production of CXCL-8.

325 ***3.4 The stimulation of CXCL8 production by SARS-CoV-2 E protein is reversed by soluble*** 326 ***rTLR2 and anti-TLR2 antibodies:***

327 The specificity of the recruitment of TLR2 pathway by E protein was further
328 characterized in complementary assays using either soluble recombinant TLR2 (rTLR2) or
329 anti-TLR2 blocking antibodies. The results show that incubation of rTLR2 with E protein
330 before stimulation of HEK-TLR2 cells inhibit by about 50% the capacity of E protein to
331 stimulate TLR2-response as measured by the production of CXCL8. Importantly, no
332 significant CXCL8 production was obtained with rTLR2 alone (**Figure 4A**). Interestingly,
333 this latter result also indicates the absence of endotoxins in the used preparation of rTLR2. In
334 agreement with the effect of rTLR2 we showed that anti-TLR2 antibodies used at 5µg/ml,
335 inhibits by about 60% E-induced CXCL8 production (**Figure 4B**) while only a moderate
336 inhibition, less than 30%, was observed by the use of anti-TLR4 antibodies (5µg/ml), used as
337 isotype controls. We also tested the effect of LPS-RS a specific antagonist of TLR4. Used at
338 10 µg/mL, LPS-RS induced a modest inhibition of E2 induced CXCL8 production of about
339 18% (**Figure 4C**). These moderate inhibitions may be caused by the steric hindrances caused
340 by the presence of anti-TLR4 antibodies and LPS-RS.

341 Altogether, these results confirm the recruitment of TLR2 pathway by E protein as
342 demonstrated by the capacity of soluble recombinant TLR2 and anti-TLR2 antibodies to
343 strongly block the production of CXCL8 chemokine production in HEK-TLR2 cells
344 stimulated by SARS-CoV-2 E protein.

345 ***3.5 SARS-CoV-2 E protein activates NF-kB as a signature of the recruitment of TLR2*** 346 ***pathway:***

347 Activation of all TLR pathways leads to activation of the NF-kB. NF-kB is an
348 important transcription factor greatly implicated in the control of the expression of cytokines
349 genes that are involved in the immune and inflammatory responses (37, 38). The analysis of
350 the *CXCL8* promotor element sequence highlights the presence of NF-kB binding site. NF-

351 kB, a REL family member is composed of hetero or homodimers of 5 subunits including
352 RelA/p65, c-Rel, RelB, p50 and p52 (39). At the inactivated state heterodimeric NF-kB is
353 present in the cytoplasm in association with its inhibitor IκB. In order to be activated, NF-kB
354 must be phosphorylated on its subunits p65 and p50, but also on its inhibitor subunit IκB, thus
355 leading on one hand, to the nuclear translocation of P65 into the nucleus, where it binds on
356 NF-kB sites at the CXCL8 promotor element sequence, and on the other hand, on the
357 dissociation, ubiquitination and proteasomal degradation of IκB (38). Here, in our study, the
358 effect of E protein on the activation of NF-kB was evaluated by monitoring its effect on the
359 phosphorylation of the p65 subunit. To this end, HEK-TLR2 cells were stimulated during 30
360 or 60 min with E protein (1 μg/ml) or with GST or PAM₃CSK₄ as negative and positive
361 controls respectively. Both at 30 and 60 min post stimulation, E protein leads to the
362 phosphorylation of p65 (**Figure 5A lanes 3 and 4**). Only a small phosphorylation of p65 was
363 observed in unstimulated cells (**Figure 5A lane 2**) and in cells stimulated with GST protein
364 (**Figure 5, lanes 5 and 6**). As expected, a strong phosphorylation was obtained following
365 stimulation with PAM₃CSK₄ (**Figure 5A lane 7**).

366 Then, the effect of E protein on the activation of NF-kB was further characterized in a
367 more functional assay, based on the evaluation of the capacity of E protein to transactivate the
368 expression of the gene product of SEAP soluble protein placed under the control of NF-kB
369 inducible promotor. To this end, HEK-TLR2 cell line stably transfected with SEAP gene
370 under the control of NF-kB, were stimulated with various amount of E protein (1ng-100
371 ng/ml) during 15 min, 30 min or 45 min. The expression of the enzymatic activity of soluble
372 secreted SEAP protein was then measured in the cell supernatants. The obtained results
373 depicted in **Figure 5B** clearly showed a positive presence of SEAP enzymatic activity since
374 15 min of stimulation with 10ng/ml of E protein. This enzymatic activity increased in time
375 and in a dose-dependent manner at 30 min and 45 min following stimulation with the highest
376 doses of 50 ng/ml and 100 ng/ml (**Figure 5 B**). As negative control, no significant SEAP
377 enzymatic activity was observed in supernatants of unstimulated HEK-TLR2 cells (**Figure 5**
378 **B**).

379 Altogether, these results showed that SARS-CoV-2 E envelope glycoprotein is able to
380 recruit and engage TLR2 pathway leading to the activation of the transcription factor NF-kB
381 as demonstrated by the phosphorylation of p65 NF-kB subunit and the transactivation of
382 SEAP gene under the control of NF-kB promotor site.

383

384 **3.6 SARS-CoV-2 E protein activation of CXCL8 production is dependent on NF- κ B**
385 **pathway:**

386 Then we wanted to evaluate the role of NF- κ B in the control of CXCL8 production in
387 response to E stimulation in HEK-TLR2. To this end, HEK-TLR2 cell line cells were
388 previously treated during 60 min with various non-toxic concentrations (1–10 μ M) of NF- κ B
389 inhibitor Bay11-7082 before stimulation with E protein (200 ng/ml). After 18 h of culture,
390 CXCL8 production was quantified in cell supernatants. A dose-dependent inhibition of
391 CXCL8 production was obtained in the presence of Bay11-7082 demonstrating the crucial
392 role of the transcription factor NF- κ B in the control of gene expression of CXCL8 chemokine
393 (**Figure 6A**).

394 In addition to NF- κ B, the promotor element sequence of CXCL8 gene contains also
395 binding sites for additional transcription factors, including AP-1 (activating protein), CREB
396 (cAMP response element binding protein), C/EBP (CAAT/enhancer-binding protein), CHOP
397 (C/EBP homologous protein) (40) and C/EBP beta (also named NF-IL-6) (41). While NF- κ B
398 is crucial for the gene expression of CXCL8, the other transcription factors, as AP1 and
399 CREB seem to play a secondary role by acting on the stability of mRNA and synergy action
400 with NF- κ B on the expression of CXCL8 gene, thus contributing to allow an efficient
401 production of CXCL8 gene product (41, 42). The MAPkinases, including P38MAPK and
402 ERK1/2 MAPK has been reported to participate in the activation of AP1 and CREB and thus,
403 indirectly via AP1 and CREB, in the contribution of the increased expression of CXCL8 gene
404 product. Taking into account these contributions, we tested the effect of the inhibition of P38
405 MAP and ERK1/2 on the production of CXCL8 following activation of HEK-TLR2 cell line
406 by E protein. To this end, HEK-TLR2 cells were previously treated during 60 min by a non-
407 toxic concentrations of SB202190 (0.1-10 μ M) and PD98059 (1-100 μ M) as inhibitors of
408 P38MAPK and MAPK ERK1/2 respectively before treatment with E protein at 200ng/ml.
409 Both inhibitors exhibit a partial inhibitory effect reaching respectively, 55% and 70 % of
410 inhibition by SB202190 and PD98059 when used at the highest concentrations (**Figure 6B**).

411 Because P38 and ERK1/2 are activated downstream of PKC, a large family of serine
412 /threonine kinase, we also evaluated the effect of PKC on the production of CXCL8 by E
413 stimulated HEK-TLR2 cells. To this end, cells were previously treated with various
414 concentrations of R0318220, an inhibitor of all PKC isoforms, before stimulation with E
415 protein at 200 ng/ml and quantification of CXCL8 in cell supernatants as described above. No

416 evident inhibition was obtained in the presence of the PKC inhibitor Ro318220 used at 0.1
417 and 1 μ M (**figure 6B**). However, the apparent inhibition observed at 10 μ M of the inhibitor is
418 further related to the cytotoxic effect of 10 μ M concentration of RO318220 as evaluated by the
419 cytotoxicity assay measuring LDH release, a signature of cell death (data not shown).

420 Taken together, our results demonstrated the direct physical interaction between the E
421 envelope protein of SARS-CoV-2 and the TLR2. This interaction engages the activation of
422 TLR2 pathway leading to the activation of the transcription factor NF- κ B which seems to
423 play, in contrast to ERK1/2 and P38 MAP kinases, a major role in the production of CXCL8
424 chemokine.

425

426

427

428 **4. Discussion**

429 Recent work by Zheng and colleagues provided genetic evidence that TLR2 pathway
430 contributes to overwhelming production of inflammatory cytokine production (particularly
431 TNF- α , IL-6, IFN- γ) during infection by SARS-CoV-2 and other β -coronaviruses, following
432 recognition of E envelop protein (31). In light of this recent finding, our study provides
433 further characterization of E – TLR2 interaction. Specifically, our results demonstrate that
434 SARS-CoV-2 E envelope protein interacts physically in a dose-dependent manner with
435 soluble recombinant TLR2 receptor but also with cell membrane TLR2 of primary human
436 monocytes and macrophages. Additionally, our findings show that E protein from SARS-
437 CoV-2 activates TLR2 pathway leading to the activation of the transcription factor NF- κ B
438 which seems to play a major role in the production of CXCL8 chemokine, in contrast to
439 ERK1/2 and P38 MAP-kinases whose inhibition only results in partial inhibition of CXCL8.

440 TLR2 was originally described to recognize ligands from bacterial origins (43-46) that
441 include diacyl and triacylglycerol moieties, proteins and polysaccharides. However, it is
442 currently assumed that recognition of TLR2 is not limited to bacterial ligand but concern a
443 broader set of molecules including viral proteins (review in (47)). These TLR2 viral ligands
444 include Glycoprotein B of Cytomegalovirus, hepatitis C core and NS3 Protein, and
445 hemagglutinin (H) of measles virus (47). Thus, E protein from SARS-CoV-2 extend the list of
446 viral TLR2 ligands. The diversity of molecules recognized by the receptor TLR2 may be
447 licensed by its capacity to form heterodimer with TLR1, TLR6 or TLR10 and to benefit from
448 the help of additional cofactors including CD14 and CD36 (47). However, the involvement of
449 TLR2 in the interaction with E protein raises a number of questions. Crystallographic studies
450 of the complex between TLR2/TLR1 and its tri-acylated lipopeptides ligands PAM₃CSK have
451 allowed to determine the sites of interaction between TLR2/TLR1 with their ligands
452 PAM₃CSK (48). The structures of the lipopeptide TLR2 ligands, PAM₃CSK and PAM₂CSK
453 contain 3 and 2 lipid chains respectively. By interacting with the hydrophobic pocket of
454 TLR2, these lipid chains allow heterodimerization of TLR2/TLR1 by PAM₃CSK and
455 TLR2/TLR6 by PAM₂CSK and the recruitment of downstream adapters including
456 Mal/Myd88, thus allowing to the activation of the TLR2 pathway (48). It is therefore
457 important to question how the E protein of SARS-CoV-2, which does not have a lipid tail, can
458 interact and activate the TLR2 pathway. Indeed, the analysis of the primary structure of the E
459 protein reveals two hydrophilic regions in the N and C terminal parts of the molecule
460 separated by a large hydrophobic domain which could present an affinity for the hydrophobic

461 pocket of TLR2. In addition, it has been reported that E protein also exists in the form of
462 homo-oligomeric multimers (15, 49, 50) which by interacting with the hydrophobic pockets
463 of TLR2, TLR1 and TLR6 could bridge the formation of heterodimers of TLR2/TLR1, or
464 TLR2/TLR6 and even of homodimers of TLR2/TLR2. Thus, further structural research
465 studies are needed to confirm these hypotheses. Our data showing that PAM₃CSK and
466 PAM₂CSK synthetic ligands interfere with E-TLR2 binding, suggest that E protein and
467 PAM₂CSK/PAM₃CSK bind TLR2 on partially overlapping sites.

468 In our study, we demonstrated a direct physical binding of E protein to TLR2 in a
469 solid phase binding assay. However, this assay is not informative about the functionality of
470 this interaction, nor it does not indicate if it induced structural rearrangements or
471 oligomerizations of TLR2. But, our findings showing that E protein is also able to bind to cell
472 membrane TLR2 of primary monocytes and macrophages, to activate the transcription NF- κ B
473 and to stimulate the production of CXCL8 chemokine represent strong arguments in favour of
474 the capability of E protein to recruit and engage TLR2 pathway.

475 Activation of TLR2 light a diverse number of intracellular signalling pathways that
476 culminate in transcription of several immunity related genes including pro-inflammatory
477 cytokines and chemokines with important role in shaping innate and adaptive immune
478 response, as well as tissue homeostasis. Our data show that E protein activates NF- κ B and
479 demonstrates that this activation is essential for CXCL8 production in HEK-TLR2 cell line.
480 The partial inhibition obtained in the presence of P38 and ERK1/2 MAPkinases inhibitors is
481 in line with the secondary role of these pathways, involved in the activation of the AP1 and
482 CREB transcription factors in the CXCL8 gene expression (41, 42).

483 Activation of TLR pathway by viruses play a mitigated role and triggers either
484 immune protection or pathogenesis of infections (51, 52). For example, the use of animal
485 model elegantly exemplifies that TLR7-dependent type I interferon production by
486 plasmacytoid dendritic cells (pDCs) confers protection against mouse hepatitis virus (MHV)
487 viral infection (53). Similarly, type I interferon production was also observed following pDCs
488 interaction with SARS-CoV (53) and SARS-CoV-2 (54). Accordingly, in order to escape
489 from TLR-mediated immunity, viruses have developed several strategies to interfere with
490 signal transduction downstream of TLR pathways (52, 55). In contrary, dysregulated
491 activation of TLR pathway has been associated with enhanced pathogenesis. This is the case
492 for TLR4 pathway which is involved in pathogenesis of IAV, EBOV, and DENV infections

493 while treatment with TLR4 antagonists (Eritoran) reduced cytokine/chemokine production
494 and alleviate disease symptoms (56). Other viruses are taking advantage of TLR pathway to
495 their own benefits. Our group and other have shown that HIV-1, through its Tat protein,
496 activates TLR4 pathway leading to the upregulation of several immunosuppressive factors
497 including IL-10, PD-L1 and IDO-1 (35, 57-59). This is also the case for measles virus which
498 subvert TLR2 pathway by its hemagglutinin (H) protein in order to upregulate the expression
499 of its own entry receptor CD150 (60). In the case of SARS-CoV-2, data from Zheng and
500 colleagues suggested that TLR2 pathway is involved in disease pathogenesis rather than viral
501 control (31).

502 Although, the exact pathway of the COVID-19 pathogenesis is still unknown, recent
503 data demonstrated that elevated levels of pro-inflammatory cytokines in serum, including
504 CXCL8, is associated with enhanced disease pathogenesis and mortality. Accordingly,
505 inflammatory mediators are promising therapeutic targets to alleviate COVID-19
506 pathogenesis (20, 61-63). Thus, understanding the molecular determinants responsible for
507 inflammatory cytokine production in the course of SARS-CoV-2 infection could provide
508 future therapeutic targets. Several SARS-CoV-2 components have been described to trigger
509 inflammatory cytokine production including detection of viral RNA by MDA-5 (64), TLR8
510 (65) and TLR7 (53, 54), activation of ACE-2 by spike (S) protein in epithelial cells (66) and
511 activation of TLR2 by E protein (32). However, the relative contribution of each pathway in
512 immune protection or pathogenesis warrants further studies. It should be noted that the work
513 of Zheng et al showed that unlike the E protein, the S protein does not seem to induce a
514 significant inflammatory reaction (31). This difference underlines the importance of
515 considering the E protein as a therapeutic target. Our findings showed that E protein induced
516 CXCL8 production in TLR2- and NF- κ B dependent manner when tested in HEK-TLR2 cell
517 line model. Thus, this model provides an important tool that could be used to screen
518 antagonist compounds which can be used as antiviral drugs. The production of CXCL8, a
519 known neutrophil chemoattractant, is consistent with the reports describing a high circulating
520 neutrophil number and associated injury in the airway and lung tissues in COVID-19 patients
521 (67, 68). Regarding the pathological deleterious effect of CXCL8 in COVID-19 patients, we
522 could consider targeting protein E for therapeutic purposes, either by immunotherapy
523 approaches by administering neutralizing anti-E antibodies to COVID-19 patients in intensive
524 care units (ICU), or by vaccine approach by combining protein E as an immunogen in future
525 vaccine candidates against COVID-19. Indeed, E protein is one of the most conserved in

526 coronaviruses (Lbachir Benmohamed, personal communication), and could be associated
527 with a crucial function essential for one of the crucial stages of the viral cycle or for the
528 pathogenicity of the virus.

529 **References:**

- 530 1. **Hu B, Guo H, Zhou P, Shi ZL.** 2021. Characteristics of SARS-CoV-2 and COVID-19. *Nature*
531 *reviews Microbiology* **19**:141-154.
- 532 2. **Huang Y, Yang C, Xu XF, Xu W, Liu SW.** 2020. Structural and functional properties of SARS-
533 CoV-2 spike protein: potential antiviral drug development for COVID-19. *Acta*
534 *pharmacologica Sinica* **41**:1141-1149.
- 535 3. **Letko M, Marzi A, Munster V.** 2020. Functional assessment of cell entry and receptor usage
536 for SARS-CoV-2 and other lineage B betacoronaviruses. *Nature microbiology* **5**:562-569.
- 537 4. **Schoeman D, Fielding BC.** 2019. Coronavirus envelope protein: current knowledge. *Virology*
538 *journal* **16**:69.
- 539 5. **Kuo L, Hurst KR, Masters PS.** 2007. Exceptional flexibility in the sequence requirements for
540 coronavirus small envelope protein function. *Journal of virology* **81**:2249-2262.
- 541 6. **Baudoux P, Carrat C, Besnardeau L, Charley B, Laude H.** 1998. Coronavirus pseudoparticles
542 formed with recombinant M and E proteins induce alpha interferon synthesis by leukocytes.
543 *Journal of virology* **72**:8636-8643.
- 544 7. **Venkatagopalan P, Daskalova SM, Lopez LA, Dolezal KA, Hogue BG.** 2015. Coronavirus
545 envelope (E) protein remains at the site of assembly. *Virology* **478**:75-85.
- 546 8. **DeDiego ML, Alvarez E, Almazan F, Rejas MT, Lamirande E, Roberts A, Shieh WJ, Zaki SR,**
547 **Subbarao K, Enjuanes L.** 2007. A severe acute respiratory syndrome coronavirus that lacks
548 the E gene is attenuated in vitro and in vivo. *Journal of virology* **81**:1701-1713.
- 549 9. **Ortego J, Ceriani JE, Patino C, Plana J, Enjuanes L.** 2007. Absence of E protein arrests
550 transmissible gastroenteritis coronavirus maturation in the secretory pathway. *Virology*
551 **368**:296-308.
- 552 10. **Netland J, DeDiego ML, Zhao J, Fett C, Alvarez E, Nieto-Torres JL, Enjuanes L, Perlman S.**
553 2010. Immunization with an attenuated severe acute respiratory syndrome coronavirus
554 deleted in E protein protects against lethal respiratory disease. *Virology* **399**:120-128.
- 555 11. **Lim KP, Liu DX.** 2001. The missing link in coronavirus assembly. Retention of the avian
556 coronavirus infectious bronchitis virus envelope protein in the pre-Golgi compartments and
557 physical interaction between the envelope and membrane proteins. *The Journal of biological*
558 *chemistry* **276**:17515-17523.
- 559 12. **Corse E, Machamer CE.** 2000. Infectious bronchitis virus E protein is targeted to the Golgi
560 complex and directs release of virus-like particles. *Journal of virology* **74**:4319-4326.
- 561 13. **Mortola E, Roy P.** 2004. Efficient assembly and release of SARS coronavirus-like particles by a
562 heterologous expression system. *FEBS letters* **576**:174-178.
- 563 14. **DeDiego ML, Nieto-Torres JL, Jimenez-Guardeno JM, Regla-Nava JA, Castano-Rodriguez C,**
564 **Fernandez-Delgado R, Usera F, Enjuanes L.** 2014. Coronavirus virulence genes with main
565 focus on SARS-CoV envelope gene. *Virus research* **194**:124-137.
- 566 15. **Nieto-Torres JL, Verdia-Baguena C, Jimenez-Guardeno JM, Regla-Nava JA, Castano-**
567 **Rodriguez C, Fernandez-Delgado R, Torres J, Aguilera VM, Enjuanes L.** 2015. Severe acute
568 respiratory syndrome coronavirus E protein transports calcium ions and activates the NLRP3
569 inflammasome. *Virology* **485**:330-339.
- 570 16. **Kindler E, Thiel V.** 2016. SARS-CoV and IFN: Too Little, Too Late. *Cell host & microbe* **19**:139-
571 141.
- 572 17. **Kim YM, Shin EC.** 2021. Type I and III interferon responses in SARS-CoV-2 infection.
573 *Experimental & molecular medicine* **53**:750-760.
- 574 18. **Vanderbeke L, Van Mol P, Van Herck Y, De Smet F, Humblet-Baron S, Martinod K, Antoranz**
575 **A, Arijs I, Boeckx B, Bosisio FM, Casaer M, Dauwe D, De Wever W, Dooms C, Dreesen E,**
576 **Emmaneel A, Filtjens J, Gouwy M, Gunst J, Hermans G, Jansen S, Lagrou K, Liston A, Lorent**
577 **N, Meersseman P, Mercier T, Neyts J, Odent J, Panovska D, Penttila PA, Pollet E, Proost P,**
578 **Qian J, Quintelier K, Raes J, Rex S, Saeys Y, Sprooten J, Tejpar S, Testelmans D, Thevissen K,**
579 **Van Buyten T, Vandenhoute J, Van Gassen S, Velasquez Pereira LC, Vos R, Weynand B,**

- 580 **Wilmer A, Yserbyt J, Garg AD, et al.** 2021. Monocyte-driven atypical cytokine storm and
581 aberrant neutrophil activation as key mediators of COVID-19 disease severity. *Nature*
582 *communications* **12**:4117.
- 583 19. **Channappanavar R, Perlman S.** 2017. Pathogenic human coronavirus infections: causes and
584 consequences of cytokine storm and immunopathology. *Seminars in immunopathology*
585 **39**:529-539.
- 586 20. **Karki R, Sharma BR, Tuladhar S, Williams EP, Zalduondo L, Samir P, Zheng M, Sundaram B,**
587 **Banoth B, Malireddi RKS, Schreiner P, Neale G, Vogel P, Webby R, Jonsson CB, Kanneganti**
588 **TD.** 2021. Synergism of TNF-alpha and IFN-gamma Triggers Inflammatory Cell Death, Tissue
589 Damage, and Mortality in SARS-CoV-2 Infection and Cytokine Shock Syndromes. *Cell* **184**:149-
590 168 e117.
- 591 21. **Jose RJ, Manuel A.** 2020. COVID-19 cytokine storm: the interplay between inflammation and
592 coagulation. *The Lancet Respiratory medicine* **8**:e46-e47.
- 593 22. **Odak I, Barros-Martins J, Bosnjak B, Stahl K, David S, Wiesner O, Busch M, Hoepfer MM,**
594 **Pink I, Welte T, Cornberg M, Stoll M, Goudeva L, Blasczyk R, Ganser A, Prinz I, Forster R,**
595 **Koenecke C, Schultze-Florey CR.** 2020. Reappearance of effector T cells is associated with
596 recovery from COVID-19. *EBioMedicine* **57**:102885.
- 597 23. **Diao B, Wang C, Tan Y, Chen X, Liu Y, Ning L, Chen L, Li M, Wang G, Yuan Z, Feng Z, Zhang Y,**
598 **Wu Y, Chen Y.** 2020. Reduction and Functional Exhaustion of T Cells in Patients With
599 Coronavirus Disease 2019 (COVID-19). *Frontiers in immunology* **11**:827.
- 600 24. **He Z, Zhao C, Dong Q, Zhuang H, Song S, Peng G, Dwyer DE.** 2005. Effects of severe acute
601 respiratory syndrome (SARS) coronavirus infection on peripheral blood lymphocytes and
602 their subsets. *International journal of infectious diseases : IJID : official publication of the*
603 *International Society for Infectious Diseases* **9**:323-330.
- 604 25. **Kieser KJ, Kagan JC.** 2017. Multi-receptor detection of individual bacterial products by the
605 innate immune system. *Nature reviews Immunology* **17**:376-390.
- 606 26. **Broz P, Dixit VM.** 2016. Inflammasomes: mechanism of assembly, regulation and signalling.
607 *Nature reviews Immunology* **16**:407-420.
- 608 27. **Kuriakose T, Man SM, Malireddi RK, Karki R, Kesavardhana S, Place DE, Neale G, Vogel P,**
609 **Kanneganti TD.** 2016. ZBP1/DAI is an innate sensor of influenza virus triggering the NLRP3
610 inflammasome and programmed cell death pathways. *Science immunology* **1**.
- 611 28. **Zhang T, Yin C, Boyd DF, Quarato G, Ingram JP, Shubina M, Ragan KB, Ishizuka T, Crawford**
612 **JC, Tummers B, Rodriguez DA, Xue J, Peri S, Kaiser WJ, Lopez CB, Xu Y, Upton JW, Thomas**
613 **PG, Green DR, Balachandran S.** 2020. Influenza Virus Z-RNAs Induce ZBP1-Mediated
614 Necroptosis. *Cell* **180**:1115-1129 e1113.
- 615 29. **Bauernfried S, Scherr MJ, Pichlmair A, Duderstadt KE, Hornung V.** 2021. Human NLRP1 is a
616 sensor for double-stranded RNA. *Science* **371**.
- 617 30. **Gringhuis SI, Hertoghs N, Kaptein TM, Zijlstra-Willems EM, Sarrami-Forooshani R, Sprokholz**
618 **JK, van Teijlingen NH, Kootstra NA, Booiman T, van Dort KA, Ribeiro CM, Drewniak A,**
619 **Geijtenbeek TB.** 2017. HIV-1 blocks the signaling adaptor MAVS to evade antiviral host
620 defense after sensing of abortive HIV-1 RNA by the host helicase DDX3. *Nature immunology*
621 **18**:225-235.
- 622 31. **Zheng M, Karki R, Williams EP, Yang D, Fitzpatrick E, Vogel P, Jonsson CB, Kanneganti TD.**
623 2021. TLR2 senses the SARS-CoV-2 envelope protein to produce inflammatory cytokines. *Nat*
624 *Immunol* **22**:829-838.
- 625 32. **Zheng M, Karki R, Williams EP, Yang D, Fitzpatrick E, Vogel P, Jonsson CB, Kanneganti TD.**
626 2021. TLR2 senses the SARS-CoV-2 envelope protein to produce inflammatory cytokines.
627 *Nature immunology* **22**:829-838.
- 628 33. **Xie X, Muruato A, Lokugamage KG, Narayanan K, Zhang X, Zou J, Liu J, Schindewolf C, Bopp**
629 **NE, Aguilar PV, Plante KS, Weaver SC, Makino S, LeDuc JW, Menachery VD, Shi PY.** 2020. An
630 Infectious cDNA Clone of SARS-CoV-2. *Cell Host Microbe* **27**:841-848 e843.

- 631 34. **Planes R, BenMohamed L, Leghmari K, Delobel P, Izopet J, Bahraoui E.** 2014. HIV-1 Tat
632 protein induces PD-L1 (B7-H1) expression on dendritic cells through tumor necrosis factor
633 alpha- and toll-like receptor 4-mediated mechanisms. *J Virol* **88**:6672-6689.
- 634 35. **Bahraoui E, Serrero M, Planes R.** 2020. HIV-1 Tat - TLR4/MD2 interaction drives the
635 expression of IDO-1 in monocytes derived dendritic cells through NF-kappaB dependent
636 pathway. *Scientific reports* **10**:8177.
- 637 36. **Serrero M, Planes R, Bahraoui E.** 2017. PKC-delta isoform plays a crucial role in Tat-TLR4
638 signalling pathway to activate NF-kappaB and CXCL8 production. *Scientific reports* **7**:2384.
- 639 37. **Baeuerle PA, Baltimore D.** 1996. NF-kappa B: ten years after. *Cell* **87**:13-20.
- 640 38. **Badou A, Bennasser Y, Moreau M, Leclerc C, Benkirane M, Bahraoui E.** 2000. Tat protein of
641 human immunodeficiency virus type 1 induces interleukin-10 in human peripheral blood
642 monocytes: implication of protein kinase C-dependent pathway. *Journal of virology*
643 **74**:10551-10562.
- 644 39. **Li Q, Verma IM.** 2002. NF-kappaB regulation in the immune system. *Nature reviews*
645 *Immunology* **2**:725-734.
- 646 40. **Vij N, Amoako MO, Mazur S, Zeitlin PL.** 2008. CHOP transcription factor mediates IL-8
647 signaling in cystic fibrosis bronchial epithelial cells. *Am J Respir Cell Mol Biol* **38**:176-184.
- 648 41. **Hoffmann E, Dittrich-Breiholz O, Holtmann H, Kracht M.** 2002. Multiple control of
649 interleukin-8 gene expression. *J Leukoc Biol* **72**:847-855.
- 650 42. **Mukaida N, Okamoto S, Ishikawa Y, Matsushima K.** 1994. Molecular mechanism of
651 interleukin-8 gene expression. *J Leukoc Biol* **56**:554-558.
- 652 43. **Schwandner R, Dziarski R, Wesche H, Rothe M, Kirschning CJ.** 1999. Peptidoglycan- and
653 lipoteichoic acid-induced cell activation is mediated by toll-like receptor 2. *The Journal of*
654 *biological chemistry* **274**:17406-17409.
- 655 44. **Yoshimura A, Lien E, Ingalls RR, Tuomanen E, Dziarski R, Golenbock D.** 1999. Cutting edge:
656 recognition of Gram-positive bacterial cell wall components by the innate immune system
657 occurs via Toll-like receptor 2. *Journal of immunology* **163**:1-5.
- 658 45. **Brightbill HD, Libraty DH, Krutzik SR, Yang RB, Belisle JT, Bleharski JR, Maitland M, Norgard
659 MV, Plevy SE, Smale ST, Brennan PJ, Bloom BR, Godowski PJ, Modlin RL.** 1999. Host defense
660 mechanisms triggered by microbial lipoproteins through toll-like receptors. *Science* **285**:732-
661 736.
- 662 46. **Lien E, Sellati TJ, Yoshimura A, Flo TH, Rawadi G, Finberg RW, Carroll JD, Espevik T, Ingalls
663 RR, Radolf JD, Golenbock DT.** 1999. Toll-like receptor 2 functions as a pattern recognition
664 receptor for diverse bacterial products. *The Journal of biological chemistry* **274**:33419-33425.
- 665 47. **Oliveira-Nascimento L, Massari P, Wetzler LM.** 2012. The Role of TLR2 in Infection and
666 Immunity. *Frontiers in immunology* **3**:79.
- 667 48. **Jin MS, Kim SE, Heo JY, Lee ME, Kim HM, Paik SG, Lee H, Lee JO.** 2007. Crystal structure of
668 the TLR1-TLR2 heterodimer induced by binding of a tri-acylated lipopeptide. *Cell* **130**:1071-
669 1082.
- 670 49. **Torres J, Wang J, Parthasarathy K, Liu DX.** 2005. The transmembrane oligomers of
671 coronavirus protein E. *Biophysical journal* **88**:1283-1290.
- 672 50. **Pervushin K, Tan E, Parthasarathy K, Lin X, Jiang FL, Yu D, Vararattanavech A, Soong TW, Liu
673 DX, Torres J.** 2009. Structure and inhibition of the SARS coronavirus envelope protein ion
674 channel. *PLoS pathogens* **5**:e1000511.
- 675 51. **Khanmohammadi S, Rezaei N.** 2021. Role of Toll-like receptors in the pathogenesis of
676 COVID-19. *Journal of medical virology* **93**:2735-2739.
- 677 52. **Lester SN, Li K.** 2014. Toll-like receptors in antiviral innate immunity. *Journal of molecular*
678 *biology* **426**:1246-1264.
- 679 53. **Cervantes-Barragan L, Züst R, Weber F, Spiegel M, Lang KS, Akira S, Thiel V, Ludewig B.**
680 2007. Control of coronavirus infection through plasmacytoid dendritic-cell-derived type I
681 interferon. *Blood* **109**:1131-1137.

- 682 54. **Onodi F, Bonnet-Madin L, Meertens L, Karpf L, Poirot J, Zhang SY, Picard C, Puel A,**
683 **Jouanguy E, Zhang Q, Le Goff J, Molina JM, Delaugerre C, Casanova JL, Amara A, Soumelis**
684 **V.** 2021. SARS-CoV-2 induces human plasmacytoid predendritic cell diversification via
685 UNC93B and IRAK4. *The Journal of experimental medicine* **218**.
- 686 55. **Kasuga Y, Zhu B, Jang KJ, Yoo JS.** 2021. Innate immune sensing of coronavirus and viral
687 evasion strategies. *Experimental & molecular medicine* **53**:723-736.
- 688 56. **Olejnik J, Hume AJ, Muhlberger E.** 2018. Toll-like receptor 4 in acute viral infection: Too
689 much of a good thing. *PLoS pathogens* **14**:e1007390.
- 690 57. **Planes R, BenMohamed L, Leghmari K, Delobel P, Izopet J, Bahraoui E.** 2014. HIV-1 Tat
691 protein induces PD-L1 (B7-H1) expression on dendritic cells through tumor necrosis factor
692 alpha- and toll-like receptor 4-mediated mechanisms. *Journal of virology* **88**:6672-6689.
- 693 58. **Ben Haij N, Leghmari K, Planes R, Thieblemont N, Bahraoui E.** 2013. HIV-1 Tat protein binds
694 to TLR4-MD2 and signals to induce TNF-alpha and IL-10. *Retrovirology* **10**:123.
- 695 59. **Planes R, Bahraoui E.** 2013. HIV-1 Tat protein induces the production of IDO in human
696 monocyte derived-dendritic cells through a direct mechanism: effect on T cells proliferation.
697 *PloS one* **8**:e74551.
- 698 60. **Bieback K, Lien E, Klagge IM, Avota E, Schneider-Schaulies J, Duprex WP, Wagner H,**
699 **Kirschning CJ, Ter Meulen V, Schneider-Schaulies S.** 2002. Hemagglutinin protein of wild-
700 type measles virus activates toll-like receptor 2 signaling. *Journal of virology* **76**:8729-8736.
- 701 61. **Jones SA, Hunter CA.** 2021. Is IL-6 a key cytokine target for therapy in COVID-19? *Nature*
702 *reviews Immunology* **21**:337-339.
- 703 62. **Rubin EJ, Longo DL, Baden LR.** 2021. Interleukin-6 Receptor Inhibition in Covid-19 - Cooling
704 the Inflammatory Soup. *The New England journal of medicine* **384**:1564-1565.
- 705 63. **Mehta P, McAuley DF, Brown M, Sanchez E, Tattersall RS, Manson JJ.** 2020. COVID-19:
706 consider cytokine storm syndromes and immunosuppression. *Lancet* **395**:1033-1034.
- 707 64. **Rebendenne A, Valadao ALC, Tauziet M, Maarifi G, Bonaventure B, McKellar J, Planes R,**
708 **Nisole S, Arnaud-Arnould M, Moncorge O, Goujon C.** 2021. SARS-CoV-2 triggers an MDA-5-
709 dependent interferon response which is unable to control replication in lung epithelial cells.
710 *Journal of virology* doi:10.1128/JVI.02415-20.
- 711 65. **Campbell GR, To RK, Hanna J, Spector SA.** 2021. SARS-CoV-2, SARS-CoV-1, and HIV-1 derived
712 ssRNA sequences activate the NLRP3 inflammasome in human macrophages through a non-
713 classical pathway. *iScience* **24**:102295.
- 714 66. **Patra T, Meyer K, Geerling L, Isbell TS, Hoft DF, Brien J, Pinto AK, Ray RB, Ray R.** 2020. SARS-
715 CoV-2 spike protein promotes IL-6 trans-signaling by activation of angiotensin II receptor
716 signaling in epithelial cells. *PLoS pathogens* **16**:e1009128.
- 717 67. **Chen N, Zhou M, Dong X, Qu J, Gong F, Han Y, Qiu Y, Wang J, Liu Y, Wei Y, Xia J, Yu T, Zhang**
718 **X, Zhang L.** 2020. Epidemiological and clinical characteristics of 99 cases of 2019 novel
719 coronavirus pneumonia in Wuhan, China: a descriptive study. *Lancet* **395**:507-513.
- 720 68. **Qin C, Zhou L, Hu Z, Zhang S, Yang S, Tao Y, Xie C, Ma K, Shang K, Wang W, Tian DS.** 2020.
721 Dysregulation of Immune Response in Patients With Coronavirus 2019 (COVID-19) in Wuhan,
722 China. *Clinical infectious diseases : an official publication of the Infectious Diseases Society of*
723 *America* **71**:762-768.

724

725

726 **Figures legends:**

727

728 **Figure 1: Binding of SARS-CoV-2 protein to human TLR2:** (A) Soluble recombinant
729 human TLR2 (100 µl at 1 µg/ml) were coated in 96 plates. After saturation, various amounts
730 of E-GST protein (1 ng/ml-1000 ng/ml) were added for 2 hours at 37°C. TLR2 E-GST
731 complexes were revealed by a solution of anti-GST-sera follow by anti-anti-GST conjugated
732 to HRP. (B) Primary human monocytes were incubated with 0,1 to 10 µg/ml of GST or GST-
733 E SARS-CoV-2 protein. Cells were stained with anti-GST (1/1000). Data were acquired using
734 FACScalibur. One representative experiment is shown. (C) Quantification of SARS-CoV-2 E
735 protein or GST control binding to human monocytes out of from 3 different experiments
736 acquired on FACScalibur. (D) Primary human macrophages were incubated with 10 µg/ml of
737 GST or GST-E SARS-CoV-2 protein. Cells were stained with anti-GST (1/500). Images were
738 acquired using EVOS M700 microscope.

739

740 **Figure 2: PAM₂CSK₄ and PAM₃CSK₄ interfere with SARS-CoV-2 E binding to**
741 **TLR2:** The specificity of E-TLR2 interaction was evaluated by testing the capacity of TLR2
742 ligands (A) PAM₂CSK₄ (0.1-10 µM) and (B) PAM₃CSK₄ (0.1-10 µM) to inhibit this
743 interaction.

744

745 **Figure 3: E protein stimulate the production of CXCL8 chemokine in a TLR2-**
746 **dependent manner:** (A) HEK-TLR2 cell line were stimulated with E protein (200ng/ml),
747 GST (10-1000ng/ml) or GST-nef (10-1000ng/ml), or PAM₃CSK₄ (10 ng/ml). CXCL8
748 chemokine production in the cell supernatants was quantified by ELISA. (B) Production of
749 CXCL8 in cell supernatants of HEK-TLR2 cells stimulated by escalating concentrations of E
750 protein (1-300ng/ml). (C-D) Production of CXCL8 in cell supernatants of HEK-null (C),
751 HEK-TLR4 (D), cell lines stimulated with E protein (1- 100ng/ml) or with PAM₃CSK₄. (E)
752 Primary human monocytes and macrophages were stimulated with E protein (1-200ng/ml).
753 Stimulation with GST (200 ng/ml) or PAM₃CSK₄ (1000 ng/ml) were used as negative and
754 positive control respectively. After 20h of treatment cell supernatant was collected and
755 CXCL8 chemokine production in the cell supernatants was quantified by ELISA. (F) Primary
756 human macrophages were infected with NeonGreen SARS-CoV-2 virus (MOI 0.01-1).
757 Stimulation with SARS-CoV-2 E protein (10 ng/ml) or PAM₃CSK₄ (10 ng/ml) were used as
758 positive control. After 20h of treatment cell supernatant was collected and CXCL8 chemokine
759 production in the cell supernatants was quantified by ELISA.

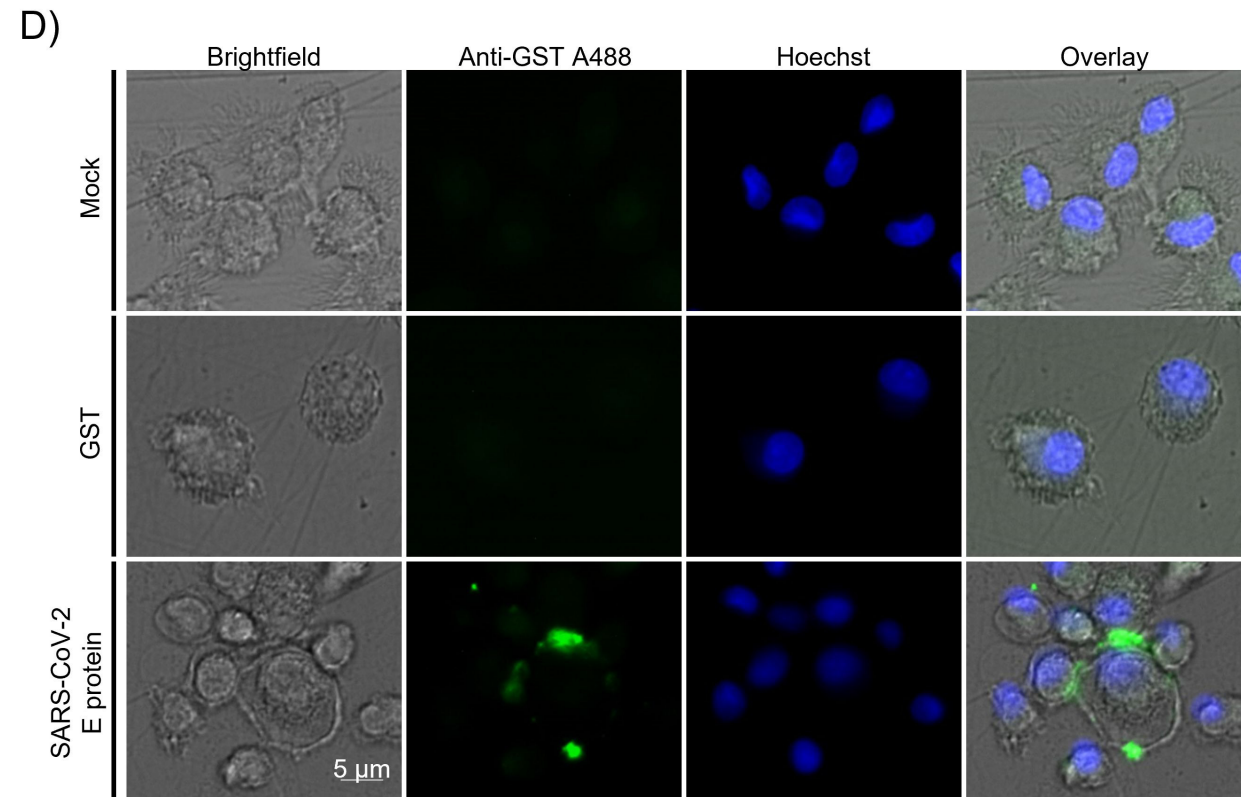
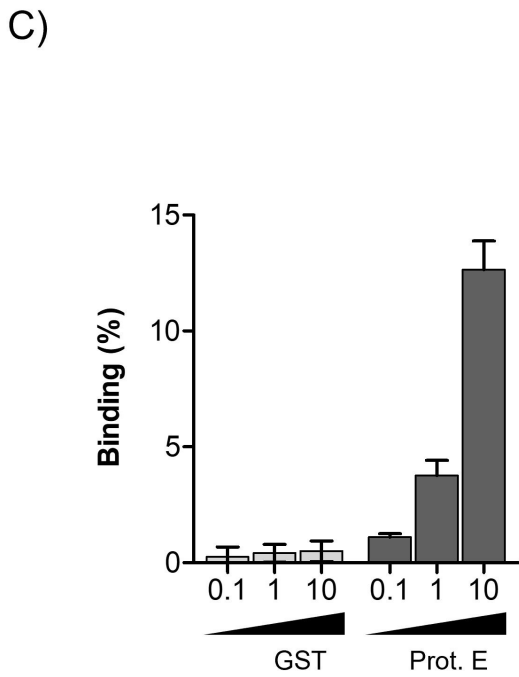
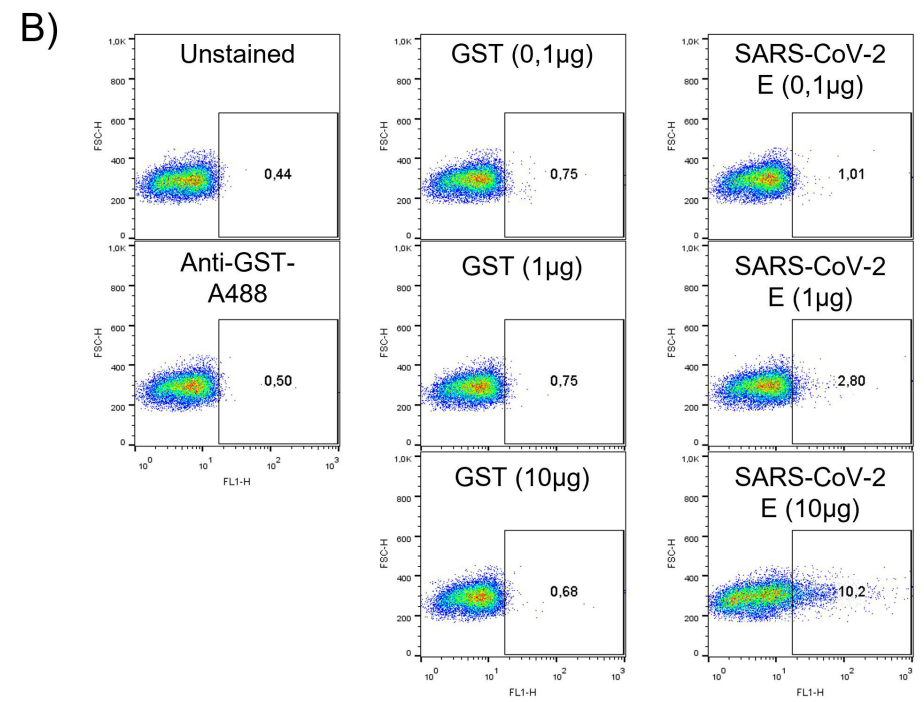
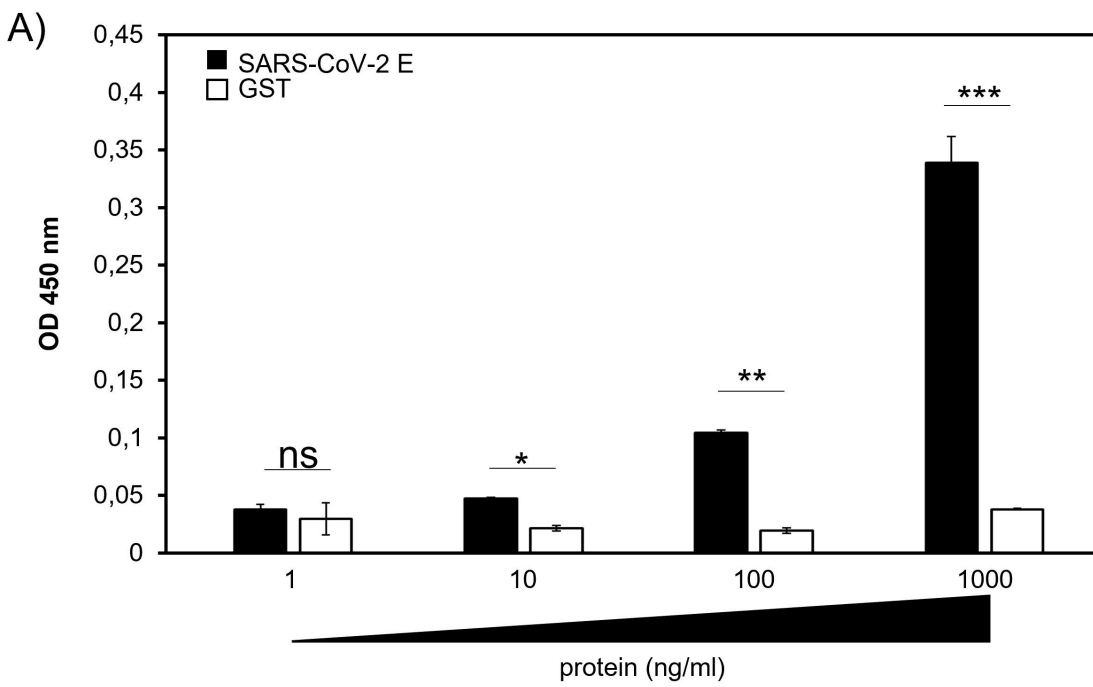
760 **Figure 4: Inhibition of E-induced CXCL8 production by soluble recombinant TLR2 and**
761 **anti-TLR2 antibodies:** HEK-TLR2 cell line were stimulated with E protein (200ng/ml) in
762 the presence or absence of recombinant TLR2 (20 ng/ml) (A), anti-TLR2 or anti-TLR4
763 antibodies (B) or LPS-RS (10 µg/ml) as control (C). HEK-TLR2 cells were also treated with
764 recombinant TLR2 (20 ng/ml) alone as control (A). After 20h of treatment cell supernatant
765 was collected and CXCL8 chemokine production in the cell supernatants was quantified by
766 ELISA.

767 **Figure 5: E protein stimulates the activation of NF-kB:** (A) HEK-TLR2 cells were
768 stimulated with E protein, GST or PAM₃CSK₄ during 30 or 60 min. Phosphorylation of P-65
769 was analysed by SDS-PAGE and western blot by using specific anti-phospho-P65 (upper
770 panel) or anti-total p65 antibodies (lower panel). (B) HEK-TLR2 cell line, stably transfected
771 with SEAP (secreted embryonic alkaline phosphatase), were treated with escalating
772 concentrations of E protein or with PAM₃CSK₄ during 15, 30 and 45 min and SEAP activity
773 was quantified in the cell supernatants.

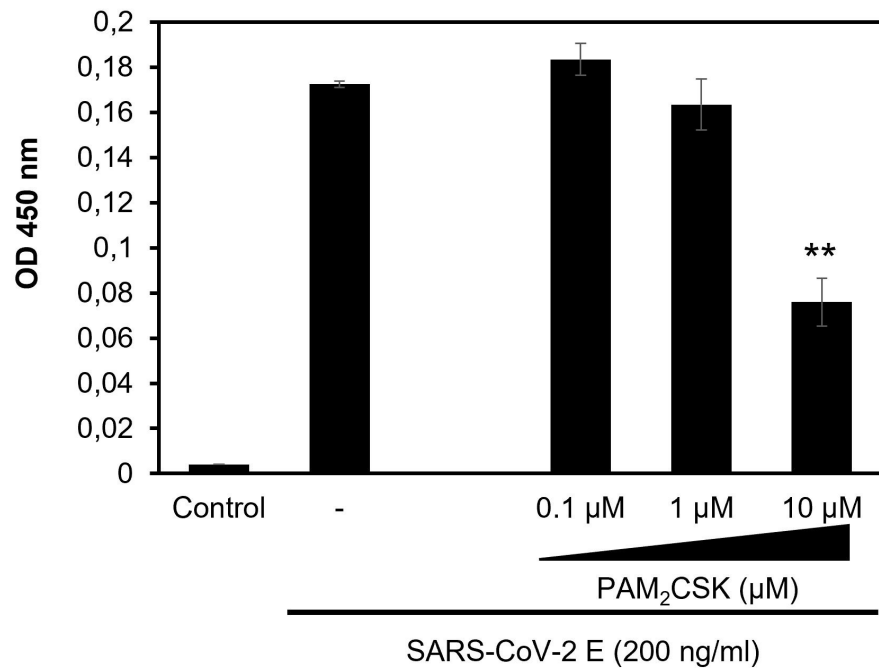
774 **Figure 6: inhibition of E- induced CXCL8 production by NF-kB inhibitor but not by**
775 **P38 and ERK1/2 MAPkinases and PKC inhibitors:** (A) inhibition of E induced-CXCL8
776 chemokine in the presence of NF-kB inhibitor. HEK-TLR2 cells were stimulated with E
777 protein (200ng/ml) in the presence of the chemical inhibitor of NF-kB Bay11 used at 1 and 10
778 µM. Production of CXCL8 in cell supernatants was quantified by ELISA. (B) HEK-TLR2
779 cells were previously treated with P38 MAP kinase inhibitor SB202190 (0.1-10µM), ERK1/2
780 inhibitor MAP kinase PD 98059 (1-100µM) or PKC inhibitor RO318220 (0.1-10µM) during
781 1 hour, before stimulation with E protein (200ng/ml). Produced CXCL8 in cell supernatants
782 was quantified by ELISA.

783

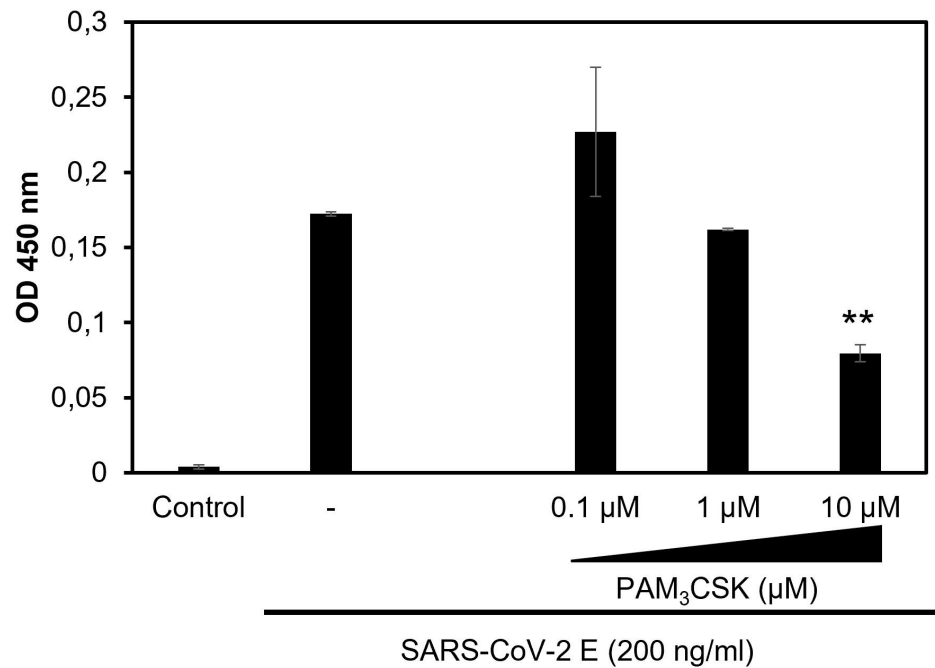
784 **Supplementary Figure S1: Infection of primary human macrophages and VeroE6 cells**
785 **with NeonGreen SARS-CoV-2 virus:** Primary human macrophages or VeroE6 cell line were
786 infected with NeonGreen SARS-CoV-2 virus (MOI 0.01-1). After 20h of infection-time cells
787 were imaged, inside BSL-3 facility, using EVOS Flöid microscope (Invitrogen). Image show
788 merge of bright field and NeonGreen fluorescence.

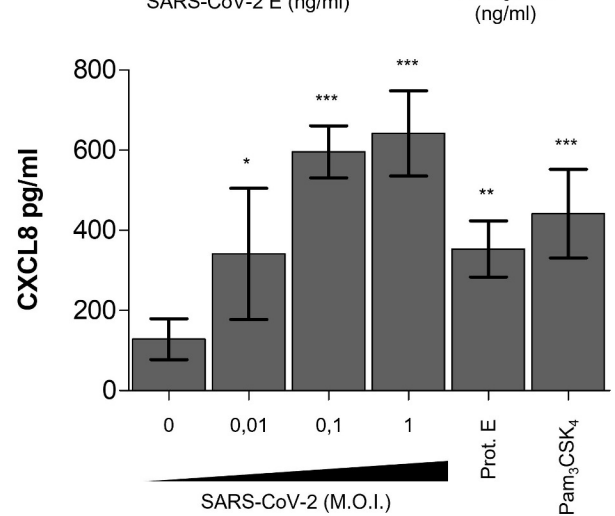
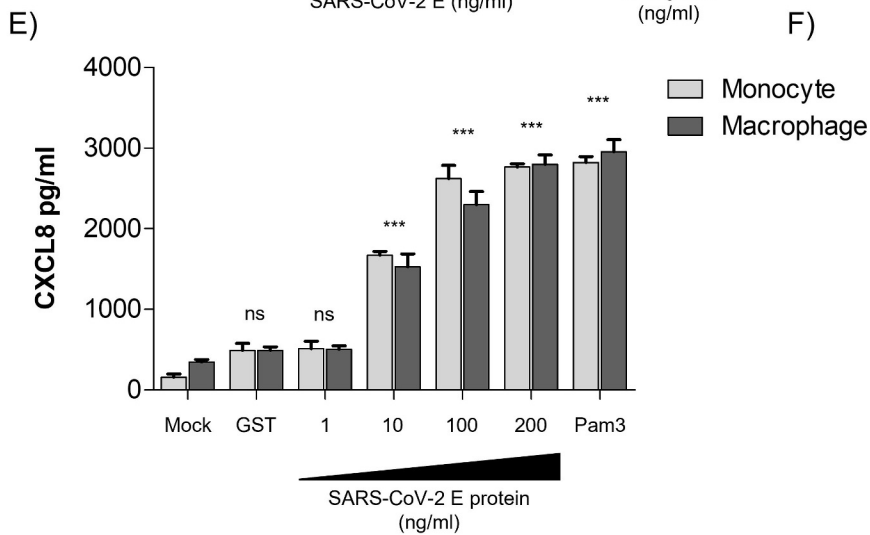
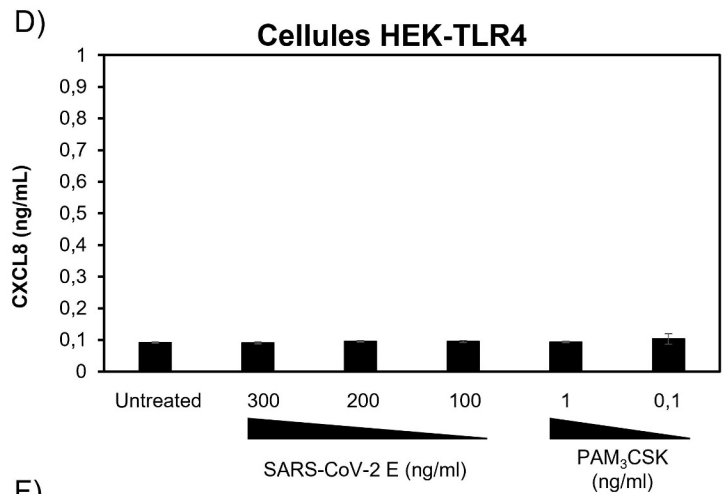
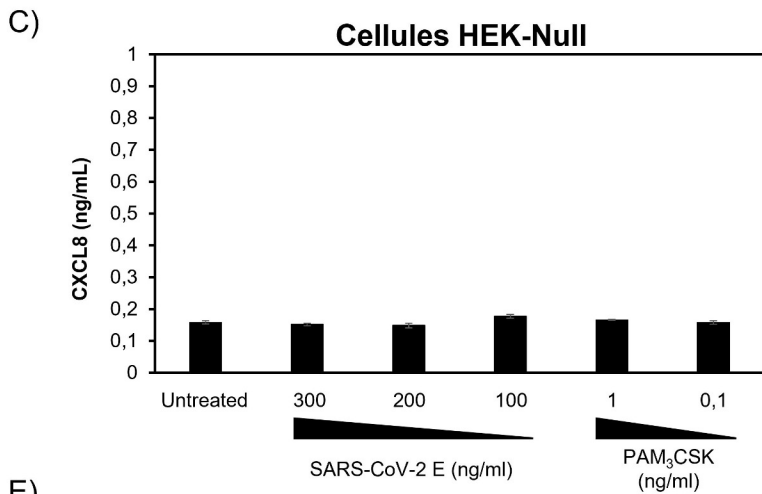
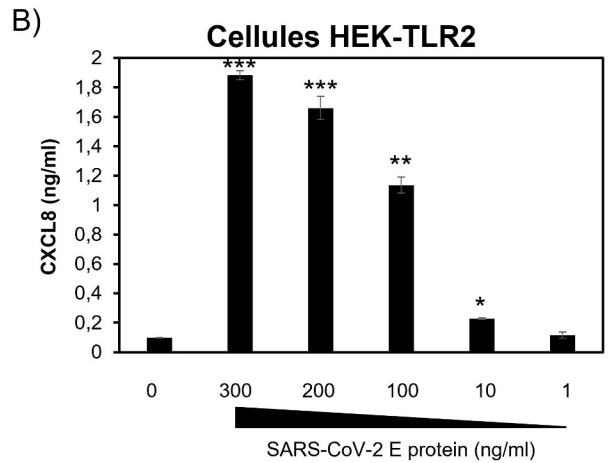
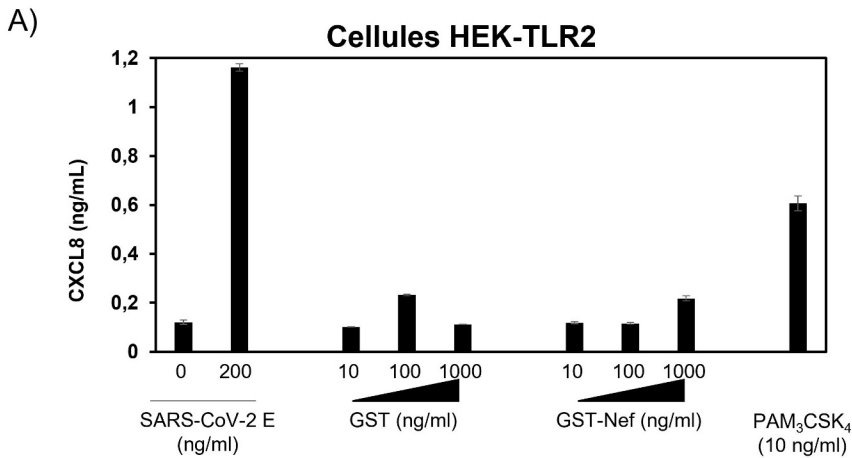


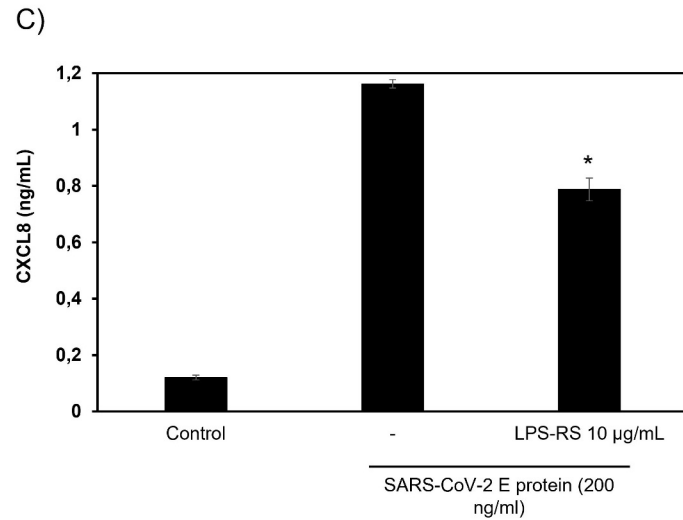
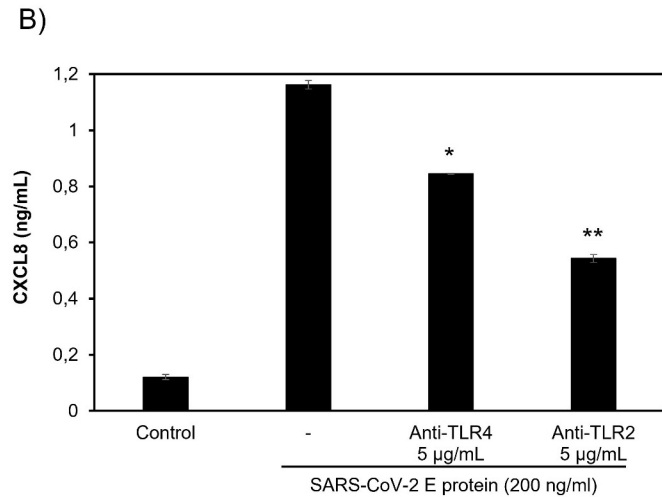
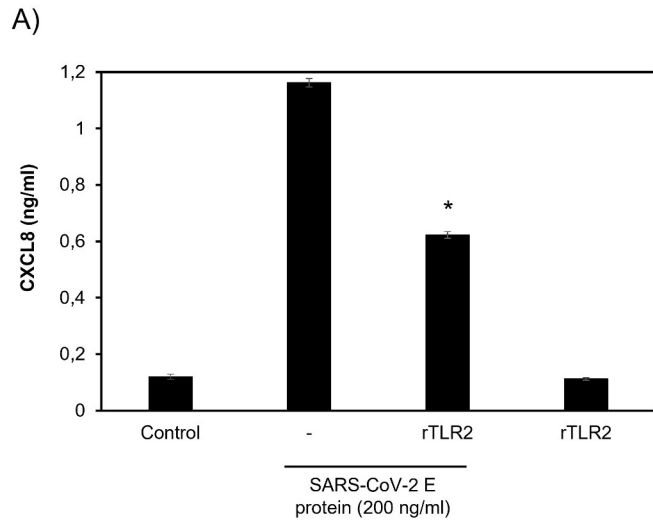
A)



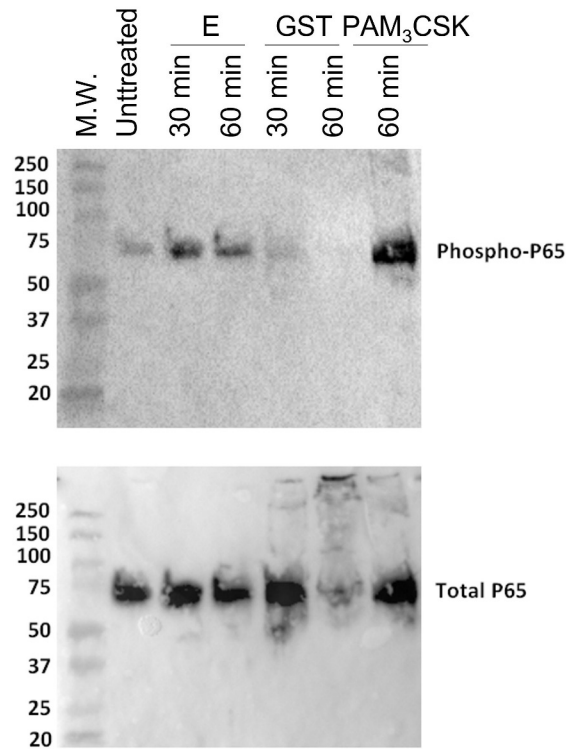
B)



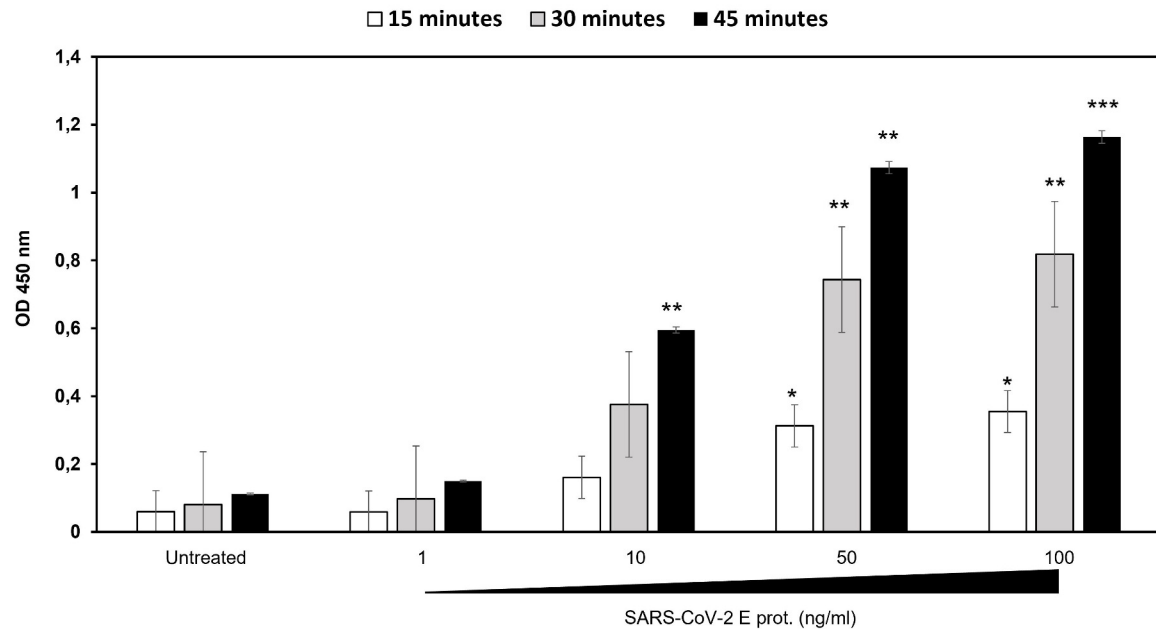




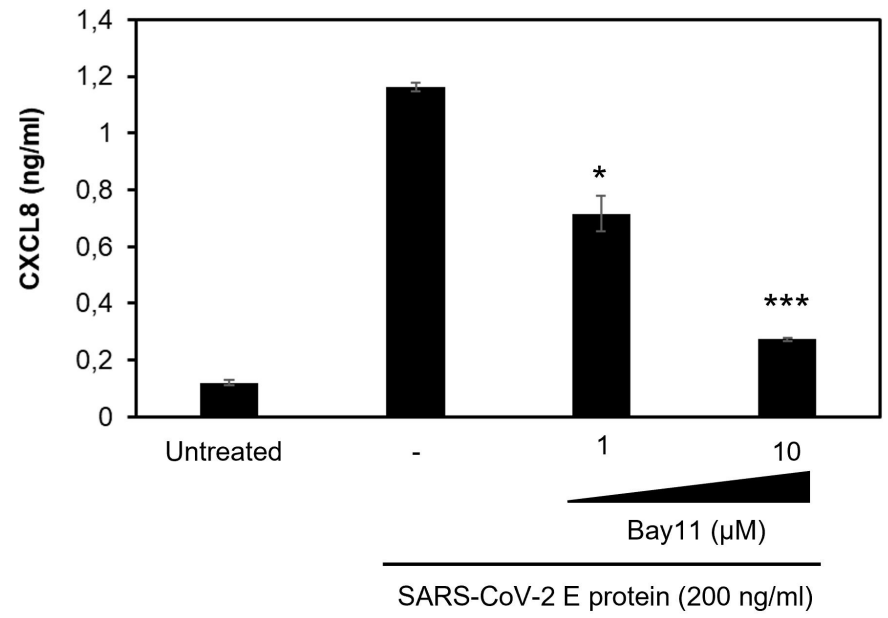
A)



B)



A)



B)

